



Webcam-based, non-contact, real-time measurement for the physiological parameters of drivers



Qi Zhang^{a,b,1}, Qingtian Wu^{b,1}, Yimin Zhou^{b,*}, Xinyu Wu^b, Yongsheng Ou^b, Huazhang Zhou^c

^a Industrial Center, Nanjing Institute of Technology, Jiangsu Province 211167, China

^b Shenzhen Institutes of Advanced Technology, Chinese Academy of Sciences, 1068 Xueyuan Avenue, Xili University Town, Shenzhen, Guangdong Province 518055, China

^c Shenzhen ChuTongZhiDa Tech.Co., Shenzhen, China

ARTICLE INFO

Article history:

Received 26 June 2016

Received in revised form 30 December 2016

Accepted 4 January 2017

Available online 5 January 2017

Keywords:

Non-contact measurement

Heart rate detection

Independent component analysis

Online monitoring

ABSTRACT

In this paper, a real-time heart rate (HR) detection system is proposed. A webcam is used to measure the HR of drivers, in order to monitor their physical activities in real time. The HR is obtained by capturing the color variations resulting from blood circulation in facial skin. Blind source separation technology, aided by the RGB color fluctuation feature in video tracking, is used for data extraction. Compared with existing commercial detection equipment, the non-contact detection method can conveniently measure the HR with acceptable accuracy, especially during driving situations that require extra precaution. Experiments in different scenarios have been performed to verify the efficacy of the proposed algorithm, which proved to be highly robust and accurate. Moreover, the developed HR detection algorithm has been implemented on the Android mobile operating system.

© 2017 Elsevier Ltd. All rights reserved.

1. Introduction

Vehicles have become an essential transportation tool in recent decades. As the number of vehicles on the road has increased, the number of traffic accidents has also inevitably increased. Statistical data from the traffic department shows that physiological and psychological factors are the primary cause of major traffic accidents [1]; these can be classified into three aspects. The first one is illness, i.e., common chronic diseases and other less severe diseases can reduce the auditory, tactile, and olfactory capabilities of drivers, and also reduce their physical reaction speed. The second factor is fatigued driving, which is the most frequent cause of traffic accidents. The third factor is the external ambient environment (i.e., temperature, humidity and road status), which could result in unfit physical conditions. Intense mental fluctuations can negatively affect the driver judgement and reactions during driving as well. Therefore, by tracking and analyzing their physiological and psychological aspects, a driver can understand and master their condition immediately so as to take precautions to prevent accidents.

Heart rate (HR), blood pressure (BP) and respiratory rate (RR) are the best indicators of a drivers's physiological state. The working condition of the cardiovascular system and level of fatigue & emotional variations can be obtained by monitoring HR, RR and other physiological parameters, so that the driving ability of the driver can be evaluated [2–4]. HR and RR are usually obtained via contact measurement methods such as electrocardiograms and fingertip photoelectric detection. The pulse waves and breathing frequency are measured through pressure sensors or electrocardiogram detection equipment connected to a specific portion of the body [5,6]. Contact measurements are normally recorded over a short period of time, in non-representable biological postures, such as sitting or lying still, which makes it difficult to capture the dynamic performance of the cardiovascular system in abnormal or particular situations [7]. Furthermore, direct contact to the skin with the detection equipment could bring discomfort and inconvenience.

Recently, methods for noninvasive measurement of HR and RR have been developed including laser Doppler [8], microwave Doppler radar [9], ultrasound [10], and thermal imaging [11,12]. However, these systems are very expensive and require complex hardware. Another method for noninvasive measurement of HR and RR is to use webcams in conjunction with image processing and blind source separation, as described by Poh [13,14]. Poh separated facial image signals via independent component analysis (ICA), and selected the heartbeat signal based on a priori knowl-

* Corresponding author.

E-mail addresses: qi.zhang@njit.edu.cn (Q. Zhang), qt.wu@sia.ac.cn (Q. Wu), ym.zhou@sia.ac.cn (Y. Zhou), xy.wu@sia.ac.cn (X. Wu), ys.ou@sia.ac.cn (Y. Ou), arthjoe@yahoo.com (H. Zhou).

¹ The first two authors contributed equally to this work.

edge. The method explores a low-cost, accurate, video-based technique for non-contact HR measurement. Wei and his colleagues [15] applied a Laplacian Eigenmap [16] to discover useful information embedded in a photoplethysmogram (PPG) signal so as to extract more accurate blood volume pulse.

Monkarezi [17] proposed an improved method that combined ICA with machine learning in a controlled human-computer interaction situation. Although the accuracy of the non-invasive measurement is increased, it can not be used in some situations such as emergency severity index triage. Lewandowska [18] used principal component analysis (PCA) to obtain the HR signal based on a small rectangular region from the face image and two color channels, which has higher computation efficiency compared to that of ICA [13]. In [19], HR can be acquired from color variations in the ROI around the mouth of the tester and the RR can be detected via shoulder movement tracking. The method has an acceptable accuracy while the tester sits in a relatively still state. Sun [20] captured the plethysmography signal via a high-speed monochrome CMOS camera focused on the palm of the participant, which can achieve an effective assessment of physiological parameters (RR, HR) if only the participants move slightly.

Some driver state monitoring systems have been proposed to detect the fatigue and drowsiness of the driver. One method is to use biomedical signals such as electrocardiograms (ECGs) and electroencephalography (EEG) to monitor the state of the driver. In [21], ECG signals are measured from the driver's palms while they grip the steering wheel, which can also be used to monitor the state of the drivers [22]. In [23], images captured by a camera are analyzed to detect physical changes in drivers, i.e., eye blinking, however, it would severely disturb driving behavior.

In summary, the mentioned methods can capture the skin color variation caused by heartbeat based on PPG. In this paper, a noninvasive, real-time webcam-based HR detection method for monitoring the driver state is proposed [24]. The ICA is used to separate and extract image components for HR measurement. Different HR measurement sceneries have been implemented to verify the effectiveness of the proposed algorithm.

The remainder of the paper is organized as follows. Section 2 introduces the basic principle of the proposed algorithm. The procedure of the method is explained in detail in Section 3. Experiments are performed in different scenarios and results are analyzed in Section 4. Conclusions and future work are discussed in Section 5.

2. Method of physiological parameter extraction

Human facial skin contains abundant capillaries. Blood volume in the vessels of the body will change according to heart rate. When the blood volume increases in the capillaries under the skin, the blood absorbs more light and the facial image becomes darker because less light is reflected from the face and vice versa [9]. This subtle variation cannot be observed by the naked eyes; however, the weak HR signals can be extracted using video image processing and the blind signal extraction method. Photoplethysmography (PPG) is a simple and low-cost optical technique that can be used to detect blood volume fluctuations through variations in transmitted or reflected light [2], which is used for physiological parameter detection.

Fig. 1 shows a diagram of non-invasive physiological parameter detection for a driver. The camera can be fixed in front of the driver, and is used to collect the facial video signals. The video is then transferred and coded so image frames can be separated, and facial recognition techniques are used to localize the face position. Afterwards, the facial images are separated into three RGB components, then each value of the components is calculated and processed

with ICA. The JADE (Joint Approximate Diagonalization of Eigenmatrices) algorithm, a low-pass filter and Fast Fourier transform (FFT) type serial algorithms are used to obtain the expected HR signals accordingly.

2.1. Facial tracking and extraction

In practice, the accuracy of facial image tracking and extraction have a significant effect on the obtainment of the HR. As for the facial image extraction, the dealt continuous frames should be kept in consistency with their location and magnitudes. The measurement algorithm is performed in real time, which requires high-speed processing capability and low calculation load in facial tracking and image extraction algorithms. Based on the requirement, a skin color based facial image extraction technique is developed, which is composed of image color space conversion, facial image location, facial characteristic identification and image extraction.

2.1.1. Image color space conversion

First, the extracted original images from the video are converted from RGB space to $YCbCr$ space to remove the correlation among color chroma signals and isolate the intensity signals, this is the most important step in visual perception. The conversion equations are shown in Eq. (1),

$$\begin{aligned} I_Y &= 0.30I_R + 0.59I_G + 0.11I_B \\ I_{Cb} &= 0.877(I_R - I_Y) \\ I_{Cr} &= 0.493(I_B - I_Y) \end{aligned} \quad (1)$$

where $I_{RGB} = \{I_R, I_G, I_B\}$ is the data matrix of the image pixels in RGB space, delegating the R, G, B components. $I_{YCbCr} = \{I_Y, I_{Cb}, I_{Cr}\}$ denotes the image data in $YCbCr$ space; I_Y is the lightness, I_{Cb} and I_{Cr} are the difference of the red and blue components from the lightness, respectively.

The video coding chip can transmit video signals to the computer for processing with a frame as one unit. Digital image frames are coded in RGB color space, where the values in the RGB components are easily disturbed by serious fluctuation in image lightness, in this case, the frames cannot be directly used for skin color judgements.

2.1.2. Facial tracking and location

Considering the skin characteristics of the Asians [1], I_{Cr} and I_{Cb} are binarized based on a pixel range, and are calculated as follows,

$$I_{Cr}/I_{Cb} = \begin{cases} 1 & 120 \leq C_r \leq 170, 100 \leq C_b \leq 150 \\ 0 & \text{else} \end{cases} \quad (2)$$

Erosion, sealing and dilation are applied to the acquired binary images to obtain the connected domain with the maximum area and length-width ratio, in accordance with the facial characteristics. The coordinates of the minimum external matrix of the connected domain, (X_1, Y_1, H_1, W_1) are calculated to roughly locate the face. Then, based on the binary facial color images, the facial region can be acquired.

2.1.3. Precise facial location

Based on the enlarged rectangle, the gray facial image data can be extracted from the gray data I_Y of the $YCbCr$ images in order to binarize the image to obtain the location of the eyes and nose. Through the coordinate calculation, the distance between the eyes and nose can be obtained and connected with a triangle, so that the middle line of the triangle (regarded as the facial middle line) can be determined.

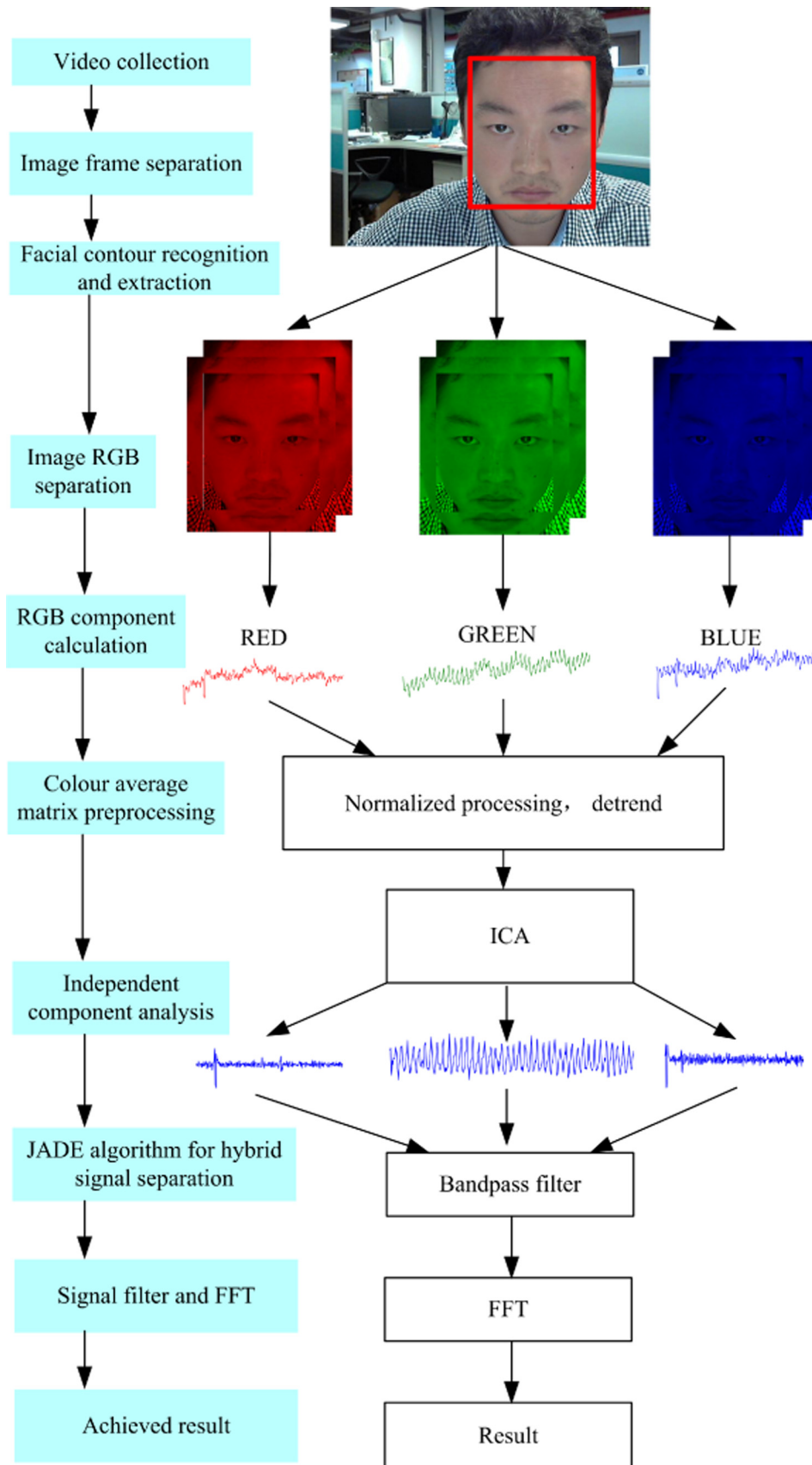


Fig. 1. The diagram of non-invasive physiological parameter detection procedure.

2.1.4. Facial image obtainment

By comparing the coordinates of the middle line from one frame to the next, it can be determined that there is only slight facial motion if the difference between two pairs of coordinates is less than the designed threshold. The last frame of the facial image is then used to track the image, in order to guarantee the stability of the location and magnitude of the image. When the difference between the middle lines in two consecutive coordinates is larger than the threshold, the coordinates of the facial image will be recalculated with a new rectangle, (X_2, Y_2, H_2, W_2) . Then the coordinates in the RGB space are relocated as $(X_1 + X_2, Y_1 + Y_2, H_2, W_2)$, and the image frames are extracted from the original RGB color space according to the rectangle location.

Once these steps are completed, the image processing unit can extract the magnitude and location of the stable facial images to prevent motion influences and environmental lightness variations on the extracted facial image. The extracted facial image obtained from the video is shown as the top image in Fig. 1, where the rectangle in the image is 70% percent of the width and full height of the original rectangle as the ROI for further calculation.

2.2. Facial image preprocessing

The average values of the RGB components of the facial images are used as the input of the blind source signal. Because of disturbances from the background environment and motion, the acquired average data could have severe fluctuation. Therefore, the noisy signals should be removed to improve the accuracy of the obtained signals, this is achieved through signal preprocessing, as shown in Fig. 2.

The averaged values of the three components in RGB space are calculated as:

$$V_i = \frac{\sum_{l=1}^n \sum_{m=1}^m (I_l)}{n \times m} \times 1000, \quad i = R, G, B \quad (3)$$

where V_i represents the average value, and the dimension of I_l is $n \times m$. Because the value of $n \times m$ is quite large compared to the magnitude of the variations in skin color, the image signal will be enlarged 1000 times for further division with higher precision. The acquired average signals, $V_{RGB} = \{V_R, V_G, V_B\}$ from red, green and blue channels are composed of 300 data with 3×300 dimension for 30 s video images. Fig. 3(a) shows the average image values.

2.2.1. Detrending

When the environmental parameters vary, the collected images will have escalation, and oblique upward or downward tendencies, which will have a negative effect on the performance of data processing tasks such as normalization, mean elimination and whitening. The detrended processing can be performed with a predefined smooth high-pass filter [28] with smoothing parameter $\lambda = 10$ and cutoff frequency = 0.059 Hz; the related dealt data wave is shown in Fig. 3(b).

2.2.2. Normalization

Blind source separation retrieves each independent component of the original signals based only on the statistical characteristics of the signals and parameters of the transmission channel. To satisfy the input requirement, normalization is adopted to transform the three color mean matrix of the images into Gaussian signals. The mean and variance values of the three components (i.e., $\{V_R(t), V_G(t), V_B(t)\}$) in the three channels are represented as the vector with $\{U_R, U_G, U_B\}$ and $\{\sigma_R, \sigma_G, \sigma_B\}$, respectively, where t delegates the time position related to the image frame of the mean values. Thus the obtained Gaussian signals are normalized with the formula,

$$X_i(t) = \frac{V_i(t) - U_i}{\sigma_i}, \quad i = R, G, B \quad (4)$$

where $X_i(t)$ is the normalized signal with zero mean and unit variance; U_i and σ_i are the mean and variance of $V_i(t)$, $i = R, G, B$. Then the normalized mean signals in the time-domain are shown in Fig. 3(c).

2.2.3. Image signal filtering

If high-frequency noise occurs in the image signals, it could be misdiagnosed as valid components. Hence, the image signals are filtered based on the frequency characteristics of the heart rate and breathing signals to reduce the disturbance. The adopted frequency of the band-pass filter is between 0.3 and 4 Hz (corresponding to heart rate [18,240]/s); the filtered image signal is depicted in Fig. 3(d).

2.3. Heart rate extraction

ICA is a computational method for separating a multivariate signal into additive subcomponents assuming that the subcomponents are all statistically independent from each other [25]. Moreover, it is a useful algorithm for reducing noise in biomedical signals [26,27]. In this study, the JADE algorithm [28] is used to process the normalized signals, as shown in Fig. 4. The signals in the Red, Green and Blue channels are depicted in the top, middle and bottom subfigures, respectively. The ICA method can further remove noise from the extracted image signals.

As shown in Fig. 4, the Red and Blue signals have chaos waves and small magnitudes, where the magnitudes of the signals are enlarged with 10^5 for clear observation. The Green signal, however, has larger magnitude fluctuation, and the frequency and magnitude have varied patterns corresponding to a heart rate pattern. It should be noted that some disturbance still exists in the green frequency power component. Therefore, a band-pass filter (128-point Hamming window, 0.6–4 Hz, heart rate 36–240) for HR extraction is used to remove the noise, in order to improve the effective signal percentage, shown in Fig. 5.

In Fig. 5, there are wave fluctuations in the heartbeat range of [50–100] (i.e., normal adult heartbeat range) in all three components. The peak values appear around 1 Hz (heart rate 60 Hz) for the Green signal, as shown in the second graph. Compared to the Red and Blue signals, the Green signal contains too many hybrid signals although energy is more concentrated there. In a comparison with other test equipment, the frequencies of the Red signal and Blue signal are obviously higher than those of the actual HR. Because the frequency of the Green signal is close to the actual frequency, it was chosen for analyzing the component containing HR information.

Then the frequency related to the peak value from the Green frequency spectrum photo in Fig. 6 is the acquired HR frequency f_h . Similarly, breathing also has an effect on the color variations; thus the range of the band-pass filter is modified (64-point Hamming window, 0.15–0.5 Hz, respiratory rate 9–30) for the purpose of acquiring the breathing frequency. FFT is used to obtain the frequency f_r related to the peak value. The obtained heart rate (HR) and respiratory rate (RR) are expressed as,

$$HR = 60 \times f_h; \quad RR = 60 \times f_r \quad (5)$$

3. Real-time HR detection system

In the designed system, the generally digital CCD is adopted and connected to a PC via a USB cable. The video code chip can generate uncompressed AVI digital video in a 24-bit RGB format, precision varied from (160×120) – (640×480) with a frame rate of 10–

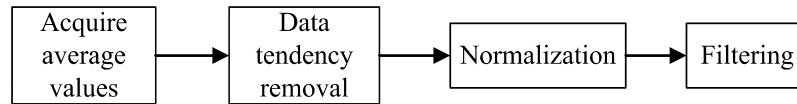


Fig. 2. Signal preprocessing.

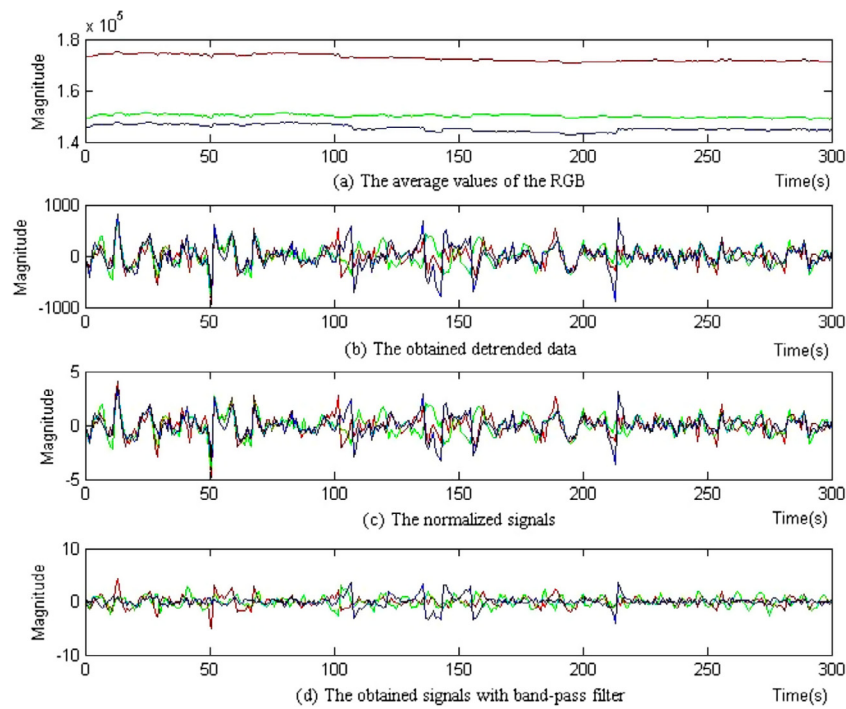


Fig. 3. Average RGB values.

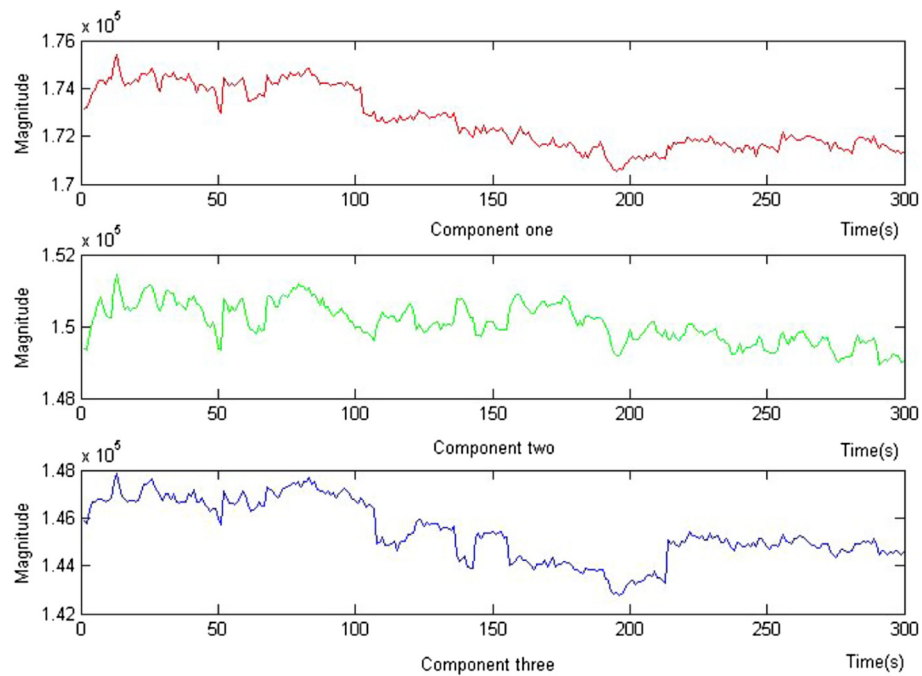


Fig. 4. Independent components of RGB image signals.

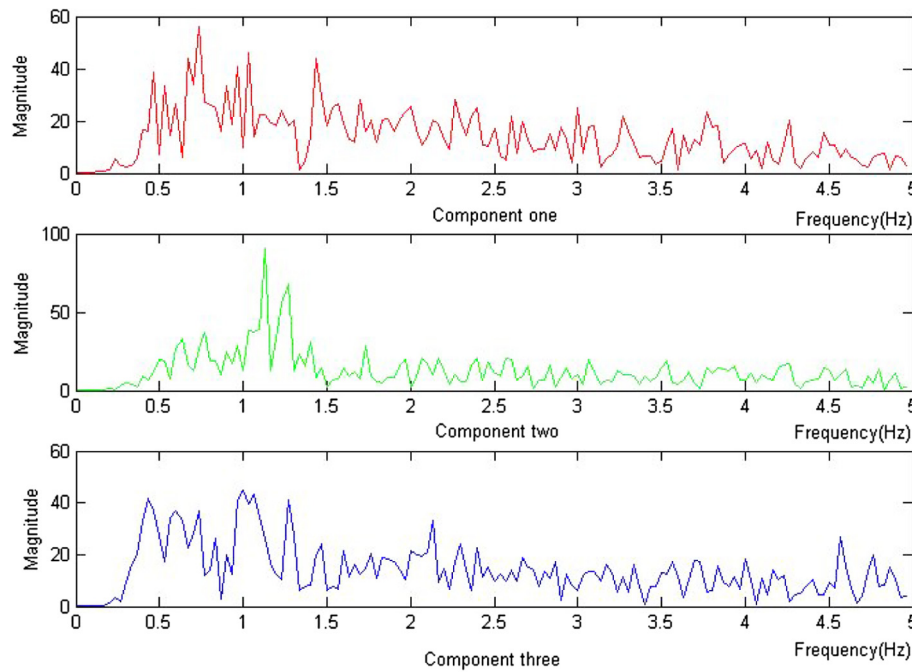


Fig. 5. Frequency power of each RGB component signals.

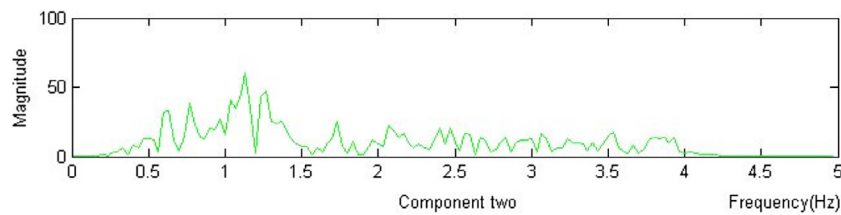


Fig. 6. Filtered green frequency power distribution component.

20/s. The data frames are transmitted to the image processing module in real time for further analysis.

The method used in [13] requires one minute of video to process to obtain the HR, which could not be used for online HR measurement. In order to detect and monitor the physiological parameters of drivers, a real time HR measurement system is designed, which consists of a video camera, a display module, an RGB raw data module, ICA and FFT processing modules and an HR & RR results display module. Fig. 7 shows the real time measurement system for HR detection; the interface and method were developed via GUI in MATLAB.

The real-time data collection procedure is described as follows. First, videos are recorded in color format at 10 frames per second. At the beginning of the measurement, $n + m$ frames are recorded in total to calculate the physiological parameters. The refresh rate is $m + 1$ frames per second; this rate is also used to control the physiological parameters recalculation. During the data update, the new input will be preprocessed to remove the noisy data via comparison. If the new data exceeds the threshold (i.e., 10 times the expectation of the stored data), it will be discarded. While each image frame is being collected, the updated stored data are separated and normalized from R , G and B channels.

The flowchart in Fig. 8 illustrates the calculation and display of physiological parameters in real time. In the detection system, the original records contain 300 frames for calculating the physiological parameters. The sampling frequency is 10 frames per second, which can be defined by the users freely according to the computer's CPU capacity.

4. Experiments and result analysis

As for the experimental settings, the platform is established in a normal indoor office environment, and a webcam (HYC-S600) is connected to a desktop computer (E5800 CPU, 3.2 GHz, 2 GB RAM, Win7 32bit). Furthermore, the HR detection algorithm was converted to the J2EE language and implemented in the Android mobile operating system. Although the resolution of the collected image recognition is lower, the processing performance and speed under Android system can be kept (Android 2.1 and above). The tester sits directly in front of the webcam at a distance of 40–50 cm. The videos are recorded in 24-bit RGB at 10 frames per second with a pixel resolution of 160×120 . The resolution of the originally collected images with HYC-S600 is with 640×480 , however, in order to increase the computation speed, the resolution of the images is compressed with 160×120 . It should be mentioned that the resolution of the dealt images can be compressed variedly, depending on whether the HR can be extracted successfully via trial and error and the computer processing performance. While the captured images are stored in the computer, it starts to process in real time, and HR can be measured every second. At the same time, finger pulse oximetry (YUYUE, YX301) is used to measure the HR of the tester for comparison.

The testers are selected randomly with different gender and ages ranging from 20–50 years old. During the experiments, testers are asked to sit still and stare at the camera, and the oxygen probe is kept on their hands. A series of experiments are performed to

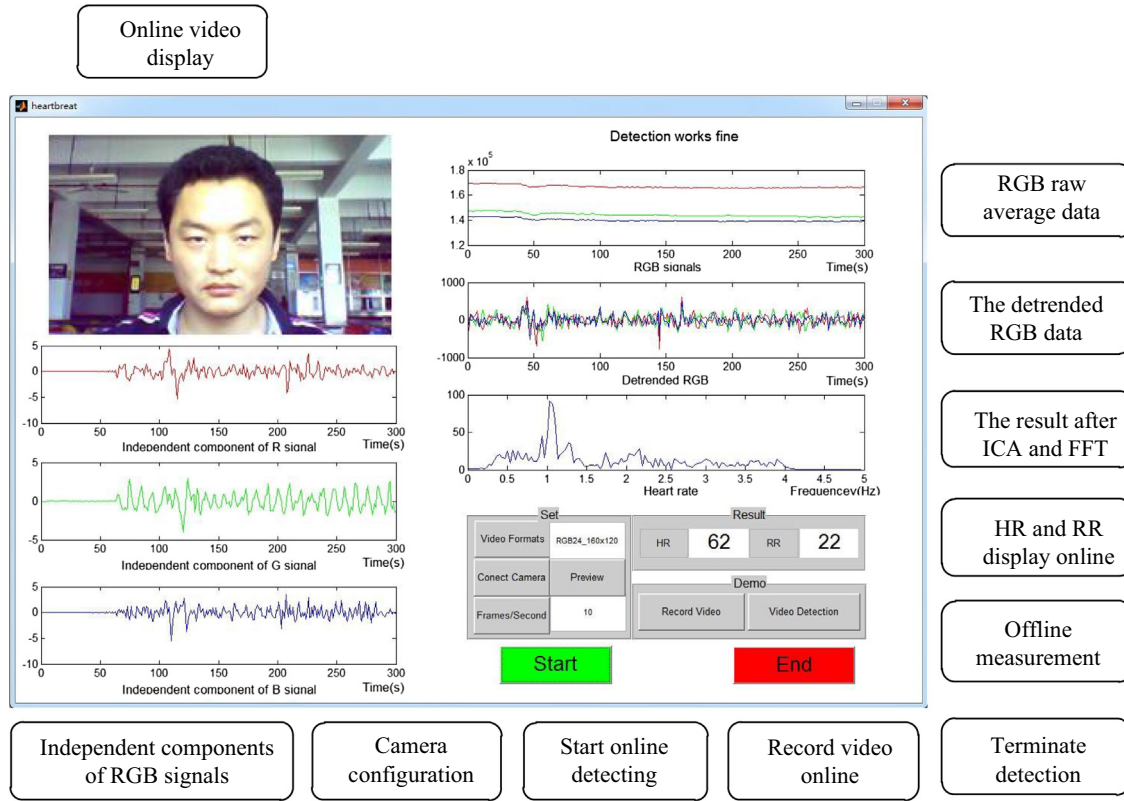


Fig. 7. Online HR measurement system.

test the performance of the acquired HR measurement via the proposed algorithm under different scenarios, i.e., varied distances between the tester and the camera, various luminosity levels and varied facial orientations.

Table 1 shows 70 s continuous HR measurements for one tester who is selected randomly from 100 testers with the 50 cm distance (i.e., chosen according to the human experience) from the camera via the proposed real-time webcam-based system. Under the circumstances with the recognized facial images of the testers, it can be seen that the slight head movement of the tester has little effect on the HR measurement. It means that the small HR variations between the oximetry and the proposed online measurement are caused due to unconscious movement from the testers or the uncomfortable clipping finger. The relative average variance (RAV) of the measurement can be calculated as,

$$AV = \frac{\sum_{i=1}^n |x_i - \bar{x}|}{n}; \quad RAV = AV / \bar{x} \times 100\% \quad (6)$$

where AV is the average variance, i.e., the summation of the absolute value of the absolute variance for individual measurement divided by the measurement times. x_i denotes each HR measurement, \bar{x} denotes the mean value of the HR measurement, and n is the number of the HR measurement. The AV and RAV of the proposed method and the oximetry are [1.5102%, 2.23%], [1.5714%, 2.46%], respectively. It can be seen that the relative average variance of the proposed method is even less than that from the commercial device. Hence, the noninvasive online HR measurement could provide good performance, and can be used as an index to monitor the state of a driver.

Table 2 shows the HR measurement results of three female and seven male participants that are selected randomly from 100 testers, ranging in age from 20–50 years old. It can be seen that small variations exist between the two types of measurements. A lot of

experiments have been performed and only 10 averaged test results are selected due to space limit. Here, the root mean squared error (RMSE) are used to evaluate the performance,

$$mean = \sum_{i=1}^n x_i \quad (7)$$

$$RMSE = \sqrt{\frac{1}{n} \sum_{i=1}^n (x_i - \bar{x})^2}$$

where x_i denotes each HR measurement.

In order to examine the effect of factors such as distance, light intensity and face orientation on the non-contact HR measurement approach, three groups of experiments are performed to verify the proposed algorithm in attempting to simulate the driving states of drivers in different scenarios.

Experiment I: In the first group of experiments, the testers are asked to vary the distances with 5 cm intervals (i.e., considering the practical situation) between themselves and the webcam, while other factors remain the same. Parts of the experimental data are list in Table 3, and the deviation (RMSE) of these measurements compared to traditional HR measurements is illustrated in Fig. 9. It is shown that non-contact measurements will provide the best performance when the distance between the tester and the webcam is around [50–55] cm. In other words, the acquired optimal distance between the tester and the webcam can be achieved or satisfied under normal driving circumstances.

Experiment II: In the second group of experiments, the effect of luminous intensity on noninvasive HR measurement is investigated. During the experiments, the tester is asked to sit still in front of the webcam at a distance of 50 cm while the luminous intensity is varied and other settings remain the same. Several test results with different luminous intensities [44, 51, 59, 81] lux (according to the human experience and normal daylight condition) via a LED lamp (SupFire M2) are shown in Table 4, and the RMSEs of

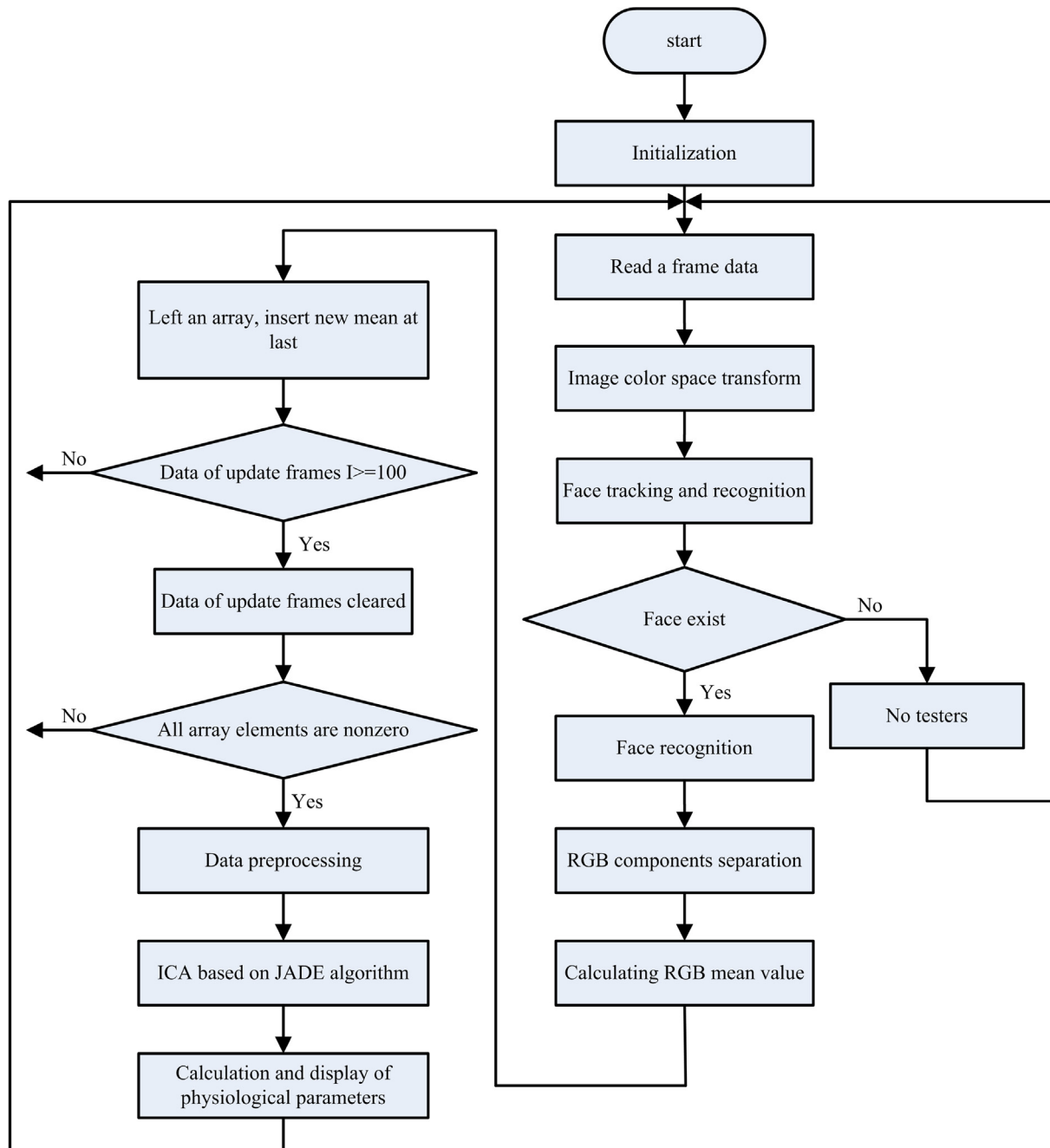


Fig. 8. Flowchart showing the calculation of real-time physiological parameters.

Table 1
Results from 70 s of continuous HR measurements.

Time (s)	10	20	30	40	50	60	70
HR using webcam (bpm)	61	64	66	65	66	63	66
HR using probe (bpm)	64	64	65	64	64	64	63

the results are depicted in Fig. 10. It can be seen that the non-contact measurement provides the best performance when the ambient luminous intensity is close to 50 Lux, which can also be guaranteed during clear daylight circumstances. As for those severe weather conditions, top light inside the vehicle should be switched on to satisfy the near optimal luminosity requirement as much as possible. Through a large amount of lab experiments

and field experiments, it can be concluded that as long as the facial images can be collected accurately in the tested luminosity range, the obtained HR measurement from the proposed algorithm can still provide guiding suggestion to the drivers.

Experiment III: In the third group of experiments, the effect of facial orientation on the noninvasive HR measurement approach is tested. Using the same experimental settings employed in the

Table 2

A series of noninvasive HR measurements.











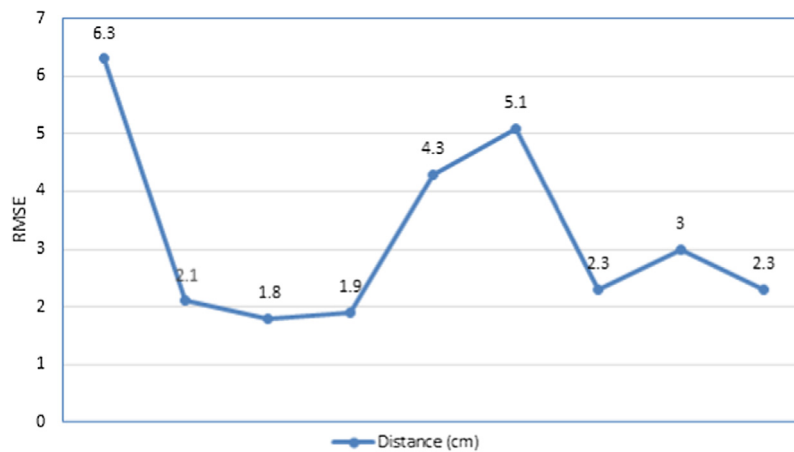
Testers										
	1	2	3	4	5	6	7	8	9	10
Contact	63	61	60	79	69	75	69	87	77	62
Noninvasive	59	61	57	74	71	74	68	86	75	63

Table 3

Effects of distance between the tester and webcam on noninvasive HR measurement.

D (cm)	Heart rate (bpm)																Mean	RMSE
40	64	64	64	64	64	72	76	64	64	64	82	82	64	66	64	64	67.2	6.3
45	64	66	66	68	60	68	62	66	66	68	68	66	66	68	66	66	65.9	2.1
50	66	68	70	68	70	70	68	68	68	66	64	70	70	68	68	66	67.8	1.8
55	66	66	66	62	70	68	68	66	66	64	68	66	66	66	64	64	66.1	1.9
60	68	68	70	72	70	72	66	66	66	68	80	78	64	64	70	70	69.2	4.3
65	70	66	60	52	74	72	72	72	70	68	68	70	70	70	64	70	68	5.1
70	68	68	74	72	74	74	72	72	72	70	68	68	68	72	68	70	70.6	2.3
75	64	62	64	66	60	60	68	64	64	64	66	68	68	66	68	70	65.6	3.0
80	62	62	64	66	66	64	70	66	66	68	64	64	62	62	62	66	64.8	2.3

**Fig. 9.** The diagram of the effect of distance on HR measurement.**Table 4**

HR measurements with different luminous intensities.

L (lux)	Heart rate data (bpm)																Mean	RMSE
44	66	64	64	62	54	52	60	62	62	62	62	60	60	60	60	60	60.7	3.7
51	66	64	62	62	60	62	62	60	60	60	60	62	62	68	62	62	62.1	2.4
59	68	66	64	64	62	60	60	62	62	58	64	62	62	64	62	62	62.3	3.2
81	60	62	64	62	60	62	52	60	62	78	62	62	62	62	62	62	62.1	5.3

second group of tests, the testers are kept 50 cm in front of the webcam in a still position. The tester will move their head around their spine, shoulders and the perpendicular of the spine and shoulders to test the maximum effective head rotation angle for the method. The experimental results are shown in Table 5, and small rotations of the head in the range of 20 degree will have little effect on the measurement performance. If the tester moves their shoulder area, 30 degree is the effective range for the online measurement approach. The scope of the rotation for the head movement is quite easy to be satisfied during driving, since the drivers would focus their attention to watch the road conditions continuously.

Field experiment: One driver willingly participated in the real-time HR measurement test in our institute (see Fig. 11). Parts of

video segments were extracted for HR measurement, and five groups of result data are listed in Table 6. The results indicate a small gap between the HR results generated by the two measurement methods. When the driver is driving, he must turn his head to observe traffic conditions, especially in front of a traffic light. During the driving experiment, it was found that a driver can keep their head in a still position for around 10 to 20 s. Therefore, the real-time heart rate system would calculate and record one heart rate every 10s for state monitoring purpose as long as the facial images can be obtained. It should be mentioned that the noninvasive HR measurement experimental results for the driver had certain measurement errors stemming from substantially varied ambient illumination. However, the results could be used to support a diagnosis index for detecting the driving status of drivers.

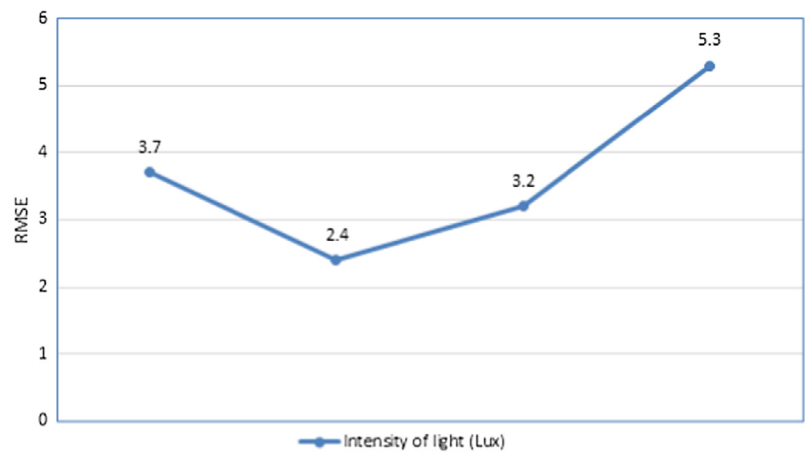


Fig. 10. Distribution of the effect of luminous intensity on the HR measurement.

Table 5
Facial orientation range for the online HR measurement.

Rotation axis	Right/up (degree)	Left/down (degree)
Spine	20	20
Shoulder	30	20
Perpendicular	20	20



Fig. 11. Real-time HR measurement for the driver.

Table 6
The real-time noninvasive HR measurement of the driver.

No	1	2	3	4	5	Mean	RMSE
Contact–HR	72	71	74	72	70	71.8	1.48
Noninvasive–HR	71	77	79	69	75	74.2	4.15



Fig. 12. HR measurement in Android environment.

Android-based HR measurement: The developed HR measurement algorithm can be transplanted in the Android development environment with Java programming language, i.e., ‘heartbeat.apk’ file (see Fig. 12). The RMSE of the HR measurement from the mobile phone and the Oximetry with 30 testers selected randomly from the 100 testers and with one tester for 100 times are 1.51 and 1.45, respectively. Therefore, the developed system on Android system can also be used as the diagnostic signal.

In the paper, the webcam is used for HR measurement under normal daylight conditions from the collected facial image via the blind source component technologies. The HR measurement procedure has been explained in details and the peak in the frequency curve corresponds to the heart beat. Compared to PPG principle, the ROI of the image has serious impact on the HR measurement but little impact on the proposed algorithm. Based on the facial image characteristics, the impact factors which would have effect on the HR measurement are analyzed. It turned out that the distance from the webcam and the tester, the ambient luminosity and the orientation of the tester are all have more and less influence on the HR measurement. However, if the proposed algorithm are used in indoor environment and the tester sits in the sat-

ified distance, lightness and orientation, the acquired result will be accurate compared to that acquired from the contact mode.

Furthermore, the optimal or near optimal distance and the orientation of the tester can be satisfied for the driver since the tester has to sit relatively still in front of the wheel while driving. Although the disturbance, i.e., road sign, would draw an attention of the drivers for a moment, the driver would turn to their normal posture quickly. The ambient luminosity has rather substantial influence on the HR measurement, which is also the general issue for any image involved applications. In this case, the drivers can turn on the top light in the vehicle when the lightness is not suitable for image capture. In summary, the proposed algorithm has the simplicity in operation, low cost and relatively accuracy advantages via commonly used webcam, especially mobile phone.

5. Conclusions

In this paper, a non-contact online HR detection method is described based on video image processing technology and blind source component technologies. It is quite suitable for automotive applications under normal driving conditions. Although the lightness variation would have certain effect on the HR measurement, the reliability of the measurement performance can still be ensured if the luminosity level kept as the normal daylight conditions. It could be used to monitor the physiological parameters of the drivers due to its low cost, non-invasive and easy implementation. Moreover, the impact of different factors, including the distance between the participant and the webcam, luminous intensities and facial orientation on the HR measurement were analyzed. The real-time HR detection system was designed with the Matlab Tool, which can be easily migrated in other operating system, i.e., Android system. Compared with the existing commercial detection equipment, the proposed non-contact detection method can measure HR with high accuracy and fast processing speed. Experimental results demonstrate that our proposed method has certain robustness to the mentioned disturbances. Future work will be carried out to investigate the heart rate variability with our proposed method to realize the fatigue monitoring of the drivers.

Acknowledgments

This work is partially supported under the Shenzhen Science and Technology Innovation Commission Project Grant Ref. CXZZ20150504171337510 and JCYJ20160510154736343, and Nanjing Institute of Technology under Grant YKJ201629. The authors would like to thank the experimental participants from the SIAT-CAS institute.

References

- [1] <http://www.chinasafety.gov.cn/zhuantibaodao/2006-05/16/content16703.htm>, 2006-05-16.
- [2] J. Allen, Photoplethysmography and its application in clinical physiological measurement, *Physiol. Meas.* 28 (2007) R1–R39.
- [3] M. Chakraborty, A.N.H. Aoyon, Implementation of computer vision to detect driver fatigue or drowsiness to reduce the chances of vehicle accident, in: 2014 International Conference on Electrical Engineering and Information & Communication Technology (ICEEICT), 2014, pp. 1–5, April.
- [4] J. Zheng, S. Hu, The preliminary investigation of imaging photoplethysmographic system, *J. Phys. Conf.* 85 (2007).
- [5] Pawan K. Baheti, H. Garudadri, An ultra low power pulse oximeter sensor based on compressed sensing, in: Sixth International Workshop on Wearable and Implantable Body Sensor Networks, 2009, pp. 144–148, June.
- [6] R. Paradiso, Wearable health care system for vital signs monitoring, in: 4th International IEEE EMBS Special Topic Conference on Information Technology Applications in Biomedicine, 2003, pp. 283–286, Apr..
- [7] J. Kranjec, S. Begus, G. Gersak, J. Drnovsek, Non-contact heart rate and heart rate variability measurements: a review, *Biomed. Signal Process. Control* 13 (2014) 102–112.
- [8] S. Ulyanov, V. Tuchin, Pulse-wave monitoring by means of focused laser beams scattered by skin surface and membranes, *Proc. SPIE, Los Angeles, CA*, vol. 1884, 1993, pp. 160–167.
- [9] E. Greneker, Radar sensing of heartbeat and respiration at a distance with applications of the technology, in: *Proc. Conf. RADAR*, Edinburgh, U.K., 1997, pp. 150–154.
- [10] S.I. Rabben, N. Stergiopoulos, et al., An ultrasound-based method for determining pulse wave velocity in superficial arteries, *J. Biomech.* 37 (10) (2004) 1615–1622.
- [11] M. Garbey, N. Sun, A. Merla, I. Pavlidis, Contact-free measurement of cardiac pulse based on the analysis of thermal imagery, *IEEE Trans. Biomed. Eng.* 54 (8) (2007) 1418–1426.
- [12] J. Fei, I. Pavlidis, Thermistor at a distance: unobtrusive measurement of breathing, *IEEE Trans. Biomed. Eng.* 57 (4) (2009) 988–998.
- [13] Ming-Zher Poh, D.J. McDuff, R.W. Picard, Advancement in noncontact, multiparameter physiological measurement using a webcam, *IEEE Trans. Biomed. Eng.* 58 (1) (2011) 7–11.
- [14] M.Z. Poh, D.J. McDuff, R.W. Picard, Non-contact, automated cardiac pulse measurements using video imaging and blind source separation, *Opt. Exp.* 18 (10) (2010) 10762–10774.
- [15] L. Wei, Y. Tian, et al., Automatic webcam-based human heart rate measurements using laplacian eigenmap, in: *ACCV'12 Proceedings of the 11th Asian Conference on Computer Vision*, vol. 7725, 2012, pp. 281–292.
- [16] M. Belkin, P. Niyogi, Laplacian eigenmaps for dimensionality reduction and data representation, *Neural Comput.* 15 (2003) 1373–1396.
- [17] H. Monkaresi, R.A. Calvo, H. Yan, A machine learning approach to improve contactless heart rate monitoring using a webcam, *IEEE J. Biomed. Health Inform.* 18 (4) (2014) 1153–1160.
- [18] M. Lewandowska, J. Ruminski, et al., Measuring pulse rate with a webcam – a non-contact method for evaluating cardiac activity, in: *Federated Conference on Computer Science and Information Systems*, 2011, pp. 405–410.
- [19] D. Shao, Y. Yang, et al., Noncontact monitoring breathing pattern, exhalation flow rate and pulse transit time, *IEEE Trans. Biomed. Eng.* 61 (11) (2014) 2760–2767.
- [20] Y. Sun, S. Hu, et al., Noncontact imaging photoplethysmography to effectively access pulse rate variability, *J. Biomed. Opt.* 18 (6) (2013) 061205.
- [21] B.G. Lee, J. Park, et al., Smartwatch-based driver vigilance indicator with kernel-fuzzy-c-means-wavelet method, *IEEE Sensors J.* 16 (1) (2016) 242–253.
- [22] U. Ha, Y. Lee, et al., A wearable EEG-HEG-HRV multimodal system with simultaneous monitoring of tES for mental health management, *IEEE Trans. Biomed. Circ. Syst.* 9 (6) (2015) 758–766.
- [23] P.P. Caffier, U. Erdmann, P. Ullsperger, Experimental evaluation of eye-blink parameters as a drowsiness measure, *Eur. J. Appl. Physiol.* 99 (2003) 319–325.
- [24] Q. Zhang, G. Xu, et al., Webcam based non-contact real-time monitoring for the physiological parameters of drivers, in: *The 4th Annual IEEE International Conference on Cyber Technology in Automation, Control and Intelligent Systems* June 4–7, Hong Kong, China, 2014.
- [25] P. Comon, Independent component analysis, a new concept?, *Signal Process* 36 (1994) 287–314.
- [26] R.R. Vazquez, H.V. Ranta, et al., wavelet denoising and discriminant analysis for EEG artefacts and noise cancelling, *Biomed. Signal Process. Control* 7 (4) (2012) 389–400.
- [27] M.R. Ram, K.V. Madhav, et al., ICA-based improved DTCWT Technique for MA reduction in PPG signals with restored respiratory information, *IEEE Trans. Instrum. Measur.* 62 (10) (2013) 2639–2651.
- [28] M.P. Tarvainen, P.O. Ranta-Aho, P.A. Karjalainen, An advanced detrending method with application to HRV analysis, *IEEE Trans. Biomed. Eng.* 49 (2) (2002) 172–175.